Annals of Botany **113**: 1235–1247, 2014
doi:10.1093/aob/mcu063, available online at www.aob.oxfordjournals.org

ANNALS OF BOTANY
Founded 1887

New insights into pioneer root xylem development: evidence obtained from *Populus trichocarpa* plants grown under field conditions

Agnieszka Bagniewska-Zadworna[1,*], Magdalena Arasimowicz-Jelonek[2], Dariusz J. Smoliński[3] and Agnieszka Stelmasik[1]

[1]*Department of General Botany,* [2]*Department of Plant Ecophysiology, Institute of Experimental Biology, Faculty of Biology, Adam Mickiewicz University, Umultowska 89, 61–614 Poznań, Poland and* [3]*Department of Cell Biology, Institute of General and Molecular Biology, Nicolaus Copernicus University, Lwowska 1, 87–100 Toruń, Poland*
** For correspondence. E-mail agabag@amu.edu.pl*

Received: 11 November 2013 Returned for revision: 20 January 2014 Accepted: 6 March 2014 Published electronically: 8 May 2014

• *Background and Aims* Effective programmed xylogenesis is critical to the structural framework of the plant root system and its central role in the acquisition and long-distance transport of water and nutrients. The process of xylem differentiation in pioneer roots under field conditions is poorly understood. In this study it is hypothesized that xylogenesis, an example of developmental programmed cell death (PCD), in the roots of woody plants demonstrates a clearly defined sequence of events resulting in cell death. A comprehensive analysis was therefore undertaken to identify the stages of xylogenesis in pioneer roots from procambial cells to fully functional vessels with lignified cell walls and secondary cell wall thickenings.
• *Methods* Xylem differentiation was monitored in the pioneer roots of *Populus trichocarpa* at the cytological level using rhizotrons under field conditions. Detection and localization of the signalling molecule nitric oxide (NO) and hydrogen peroxide (H_2O_2) was undertaken and a detailed examination of nuclear changes during xylogenesis was conducted. In addition, analyses of the expression of genes involved in secondary cell wall synthesis were performed *in situ*.
• *Key Results* The primary event in initially differentiating tracheary elements (TEs) was a burst of NO in thin-walled cells, followed by H_2O_2 synthesis and the appearance of TUNEL (terminal deoxynucleotidyl transferase-mediated dUTP nick end labelling)-positive nuclei. The first changes in nuclear structure were observed in the early stages of xylogenesis of pioneer roots, prior to lignification; however, the nucleus was detectable under transmission electron microscopy in differentiating cells until the stage at which vacuole integrity was maintained, indicating that their degradation was slow and prolonged. The subsequent sequence of events involved secondary cell wall formation and autophagy. Potential gene markers from the cinnamyl alcohol dehydrogenase (CAD) gene family that were related to secondary wall synthesis were associated with primary xylogenesis, showing clear expression in cells that undergo differentiation into TEs and in the thin-walled cells adjacent to the xylem pole.
• *Conclusions* The early events of TE formation during pioneer root development are described, together with the timing of xylogenesis from signalling via NO, through secondary cell wall synthesis and autophagy events that are initiated long before lignification. This is the first work describing experiments conducted *in planta* on roots under field conditions demonstrating that the process of xylogenesis *in vivo* might be gradual and complex.

Key words: *Populus trichocarpa*, black cottonwood, pioneer root development, programmed cell death, PCD, nitric oxide signalling, tracheary elements, cell wall synthesis, xylogenesis.

INTRODUCTION

The root system is critical to ensuring a plant's ability to cope with unfavourable soil conditions, including an inadequate water supply. Plant root systems effectively manage water absorption and rapid water transport to the shoot (Sperry *et al*., 2002). Water uptake and delivery to above-ground tissues is possible through the ability of perennial plants, and trees in particular, to develop a variety of root types. This phenomenon, which is termed heterorhizy (Noëlle, 1910; Hishi, 2007), enables the specialization of roots to perform specific biological functions (Barlow, 1993). Primary roots may be classified into (1) short and thin roots (usually up to 1 mm in diameter), which are termed fibrous, fine or feeder roots; and (2) long, fast-growing pioneer roots (of even >2 mm diameter), which form the framework of the root system and are also termed coarse, framework or skeleton roots (Kolesnikov, 1971; Lyford, 1980; Sutton and Tinus, 1983). Phenotypic plasticity allows root systems to react quickly and adapt to changing environmental conditions (Hodge, 2009). In black cottonwood, fibrous roots function in the absorption of water and nutrients, whereas pioneer roots have a greater role in transport. The rapid acquisition of transport capacity in pioneer roots is facilitated by the initiation of secondary growth and the formation of tracheary elements (TEs) that are larger and more numerous than those found in fibrous roots (Bagniewska-Zadworna *et al*., 2012). Despite the importance of acquisition of the capacity for effective xylem transport, relatively little attention has been paid to the processes that underlie xylogenesis in roots. Previous studies on the roots of woody plants focused mainly on histogenesis of the vascular system (Verdaguer and

Molinas, 1999) or on variation in the number of protoxylem groups formed and its seasonal fluctuation (Hishi and Takeda, 2005). Most studies have investigated secondary xylem formation in above-ground organs of plants, but such studies have not always considered the formation of TEs (vessels and/or tracheids), and in particular xylem fibres, which are the main component of wood (Arend and Fromm, 2003; Moreau *et al*., 2005; Courtois-Moreau *et al*., 2009; Kaneda *et al*., 2010). Our previous work (Bagniewska-Zadworna *et al*., 2012) involved the use of light and electron microscopic techniques to describe in detail the process of autophagy during formation of fully functional xylem vessels in relation to the roles played by different types of roots (fibrous and pioneer roots) of black cottonwood grown under field conditions.

Xylogenesis is a characteristic process of vessel differentiation, which results in cell death at vessel maturity in higher plants. The process is genetically programmed and is a typical example of developmental programmed cell death (PCD; Fukuda, 1996, 2000; Roberts and McCann, 2000; Elmore, 2007). Conducting an experimental assessment of both primary (TE development) and secondary (mostly fibre development) xylogenesis under field conditions is difficult. However, the process of TE formation in isolated cells has been well studied *in vitro* at the structural and molecular levels. These studies show that before plant cells enter the PCD pathway associated with xylogenesis, they must pass through several stages that lead to transformation into vessel elements (Turner *et al*., 2007). These observations have confirmed unambiguously that xylogenesis leads to the degeneration of organelles and finally to complete elimination of the protoplast (O'Brien and Thimann, 1967; Srivastava and Singh, 1972; Groover *et al*., 1997). This process is best documented by a Japanese research team (Fukuda, 2000, 2004; Kuriyama and Fukuda, 2001) for the herbaceous species *Zinnia elegans*. In that species, symptoms of initiation of individual stages of xylogenesis were identified at the structural level: these include the absence of cyclosis, changes in organelle structure, disruption of the tonoplast and, finally, complete degradation of the protoplast caused by rupture of the vacuole and the release of hydrolytic enzymes (Groover *et al*., 1997; Fukuda, 2000; Obara *et al*., 2001). However, the practical relevance of research conducted using *Z. elegans* cell suspensions, which involves the use of an appropriate set of plant hormones to induce the formation of TEs *in vitro* (Kuriyama and Fukuda, 2001), requires comparison with the results of *in vivo* studies, especially for below-ground plant organs.

Consideration of the different stages of xylogenesis requires that special attention be paid to the most conspicuous stage, namely formation of the lignified secondary cell wall and characteristic wall thickenings of TEs, as well as changes in the nucleus, demonstrating DNA degradation. Lignification is an irreversible process that is usually preceded by deposition of cellulose and non-cellulosic matrix components, such as hemicelluloses, pectins and cell wall proteins (Fukuda, 1996; Turner *et al*., 2007). Lignification of xylem secondary cell walls ensures the structural integrity of cell walls. As a waterproof phenolic heteropolymer, lignin enables xylem to transport water and solutes throughout the plant (Boyce *et al*., 2004). However, it is suggested that secondary wall deposition need not be dependent on lignin synthesis in the course of xylem differentiation *in vitro* (Kaliamoorthy and Krishnamurthy, 1998). Thus, it is essential to understand how the composition of the cell wall changes with xylogenesis *in vivo* (primary cell walls of differentiating xylem TEs vs. secondary cell walls of maturing vessels and fibres). This process includes activation of monolignol biosynthesis (Boerjan *et al*., 2003), which involves many enzymes including cinnamyl alcohol dehydrogenase (CAD), which may provide a marker of xylem differentiation. However, fragmentation of nuclear DNA is probably a better marker of the first stages of xylogenesis than increased CAD activity. Fragmentation of DNA, which is one of the main characteristics of PCD in both animals and plants (Bortner *et al*., 1995; Mittler and Lam, 1995, Obara *et al*., 2001; Nakaba *et al*., 2011), is usually analysed using either the TUNEL (terminal deoxynucleotidyl transferase-mediated dUTP nick end labelling; Groover *et al*., 1997; Groover and Jones, 1999) or comet assays (Leśniewska *et al*., 2000; Ning *et al*., 2002). After the initiation of cell degradation, the course of events that lead to cell death is usually irreversible (Yorimitsu and Klionsky, 2005) and culminates with autophagy, which involves disruption of the autophagic vacuole and release of the enzymes it contains, and the resultant acidification of the cytoplasm and subsequent digestion of all cell contents (Van Doorn and Woltering, 2005, 2010).

Our previous work chronicled the events of xylogenesis in pioneer and fibrous roots under field conditions, and provided evidence for the role of different types of autophagy (Bagniewska-Zadworna *et al*., 2012). By extending the analysis beyond simply examining tonoplast rupture at the end of autophagy, which results in cell autolysis, this previous study provided an accurate account of events that occur during primary xylem differentiation in pioneer and fibrous roots under field conditions. We hypothesized that xylogenesis in the roots of woody plants grown under field conditions is more gradual and complex than was previously described for suspension cultures forced to transdifferentiate into TEs. Therefore, on the basis of the results of our previous anatomical and cytological study (Bagniewska-Zadworna *et al*., 2012), the main aim of our present research is to undertake a comprehensive analysis to identify the subsequent stages of xylogenesis in pioneer roots from procambial cells to fully functional vessels with lignified cell walls and secondary cell wall thickenings. The ultimate goal of our research is to broaden the current knowledge of xylogenesis in woody plants. In this study, we focused on detection and localization of the signalling molecule nitric oxide (NO) and hydrogen peroxide (H_2O_2), and conducted a detailed examination of nuclear changes during xylogenesis. In addition, analyses of the expression of genes involved in secondary cell wall synthesis were performed *in situ*.

MATERIALS AND METHODS

Plant material

All experiments were performed on mature *Populus trichocarpa* Torr. & A.Gray trees growing at the experimental field site of the Institute of Dendrology, Polish Academy of Sciences in Kórnik, Poland (52°14′40″N, 17°06′27″E), the same as described in our previous work (Bagniewska-Zadworna *et al*., 2012). Observations began at least 6 months after the root boxes (rhizotrons) were installed, which allowed the soil to settle and undisturbed new roots to grow against the transparent acetate window. All observations were performed during three vegetative seasons, in June and July 2010–2012. Pioneer roots were

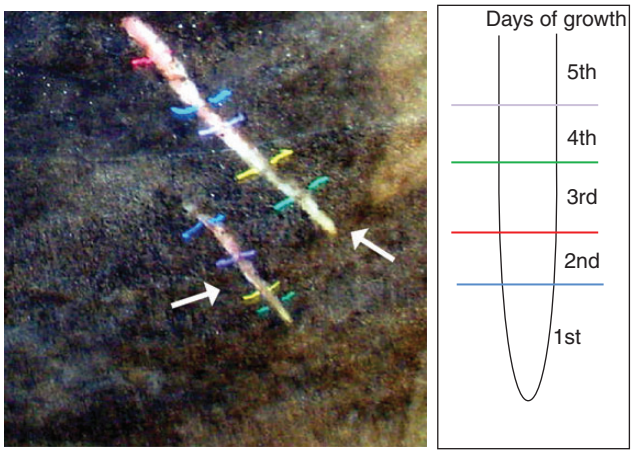

FIG. 1. Pioneer root morphology. Newly formed pioneer roots visible through the acetate window in the rhizotron and the method of tracing the daily growth of the roots.

identified in the field based on their morphology (larger diameter of pioneer roots than fibrous roots) as described earlier (Bagniewska-Zadworna *et al*., 2012). The daily rate of root growth was monitored under field conditions using the root boxes. New root growth visible on the acetate was traced daily with different coloured extrafine markers (Fig. 1). Individual pioneer roots were cut directly through the acetate at soil depths ranging from 5 to 30 cm. Rhizotrons allow roots to be observed from early stages of development without excavation, and to be sampled at a known age from the first to seventh day of root growth and divided with a razor blade into four age categories: first, second, third–fourth and fifth–seventh day of growth. Individual root segments at known age were used for further analyses.

Root anatomical studies

For histological analysis, the samples of root segments at known age were fixed immediately after harvesting in 2 % glutaraldehyde and 2 % formaldehyde (overnight with one change of solution; pH 6·8; Polysciences, Warrington, USA). The material was rinsed three times with cacodylate buffer (0·05 m; pH 6·8; Polysciences) and dehydrated in a graded ethanol series (10–100 %). It was then treated with butanol, and finally infiltrated and embedded in Paraplast Plus (melting point = 57 °C; Sigma, St Louis, MO, USA). The 12 μm thick serial sections of roots at each age category were prepared with a HM 340E rotary microtome (Microm, Walldorf, Germany). They were double-stained with Safranin O and Fast Green, and were examined using a light microscope (Axioscope A1, Carl Zeiss, Jena, Germany).

TUNEL assay

For nuclear DNA fragmentation analysis, harvested samples of pioneer roots (from the same root segments as for anatomical studies) were fixed immediately and processed as described above. The TUNEL assay measures DNA fragmentation using the terminal deoxynucleotidyl transferase (TdT)-mediated deoxyuridine triphosphate (dUTP) nick end labelling method, which involves the TdT-mediated addition of fluorescein-12-dUTP to the 3′-OH ends of fragmented DNA (TUNEL fluorescein; Roche, Indianapolis, IN, USA). Prior to the TUNEL assay, sections were hydrated in an ethanol/water series and incubated for 2 min in Triton X-100 solution (0·1 % Triton X-100 in 0·1 % sodium citrate) on ice. After rinsing the samples three times in phosphate-buffered saline (PBS), the material of each age category (at least five replicates of each) was analysed using the *in situ* Cell Death Detection (TUNEL assay) kit in accordance with the manufacturer's instructions (Roche, http://www.roche.com). Negative controls were conducted in the absence of the TUNEL enzyme. Positive controls were generated by incubating the tissue with DNase I (Roche) for 10 min at 25 °C prior to labelling. The samples were examined using a fluorescence microscope (Axiostar plus, Carl Zeiss, Jena, Germany) equipped with a digital camera, with excitation at 488 nm and emission at 515 nm. For quantitative analyses, each of the root segments was analysed on serial microtome sections to check if TUNEL-positive nuclei would appear in a different position of the same cell. For statistics, TUNEL-positive nuclei in the cells with thin unlignified cells and in the lignified cells were counted per each xylem pole of individual root segment and analysed using the Student's *t*-test in STATISTICA 10 software (StatSoft, Tulsa, OK, USA).

Transmission electron microscopy

For observation of nuclei during all stages of xylogenesis, pioneer root segments were preserved as closely as possible to their native state by fixation with 2 % glutaraldehyde and 2 % formaldehyde, and then processed in accordance with a previously described procedure (Zenkteler and Bagniewska-Zadworna, 2005). Ultrathin sections (0·1 μm) were cut with a diamond knife on an EM UC6 ultramicrotome (Leica-Reichert, Bensheim, Germany) and collected on Formvar-coated copper grids. The sections were examined with a JEM 1200 EX II transmission electron microscope (JEOL, Tokyo, Japan) at an accelerating voltage of 80 keV.

For cytological studies, at least five root segments from each age category were harvested. An average of three copper grids per sample were examined by transmission electron microscopy (TEM).

Histochemical localization of hydrogen peroxide

For detection of an oxidative burst, H_2O_2 was assayed as described by Thordal-Christensen *et al*. (1997). *In situ* peroxidase activity was detected after 60 min treatment of pioneer roots by a colour reaction with 3,3′-diaminobenzidine (DAB; Sigma) at pH 3·8. Observations were performed with CM1850 cryostat (Leica Microsystems, Nussloch, Germany) sections using an Axioscope A1 microscope (Carl Zeiss). The appearance of a red-brown colour within root cells indicated the presence of H_2O_2.

Detection of endogenous nitric oxide

The formation of NO was detected using a fluorescent 4,5-diaminofluorescein diacetate (DAF-2DA) dye as described by Floryszak-Wieczorek *et al*. (2007). Root segments were incubated for 1 h at room temperature with 10 μM DAF-2DA (Calbiochem, Darmstadt, Germany) prepared using loading buffer (10 mM Tris–HCl, pH 7·2), added from a 5 mM stock

prepared in dimethylsulfoxide. The incubation solutions were discarded, and the root segments were washed three times with fresh loading buffer to remove excess fluorophore. After several minutes, the hand-made sections were observed in 250 μL of fresh loading buffer.

A Leica TCS SP5II microscope equipped with a confocal laser scanner (Leica) was used to visualize sections, which were excited with the 488 nm line of an argon laser. Dye emissions were recorded using a 505–530 nm band-pass filter. Microscope, laser and photomultiplier settings were constant during the experiment in order to obtain comparable data. Images were processed and analysed using LAS AF (Laser Application Suite Advanced Fluorescence) software.

Fluorescent in situ *hybridization*

To prepare the probes for study of the *PoptrCAD4* and *PoptrCAD10* genes, the websites http://frodo.wi.mit.edu/primer3/ and rna.tbi.univie.ac.at/cgi-bin/RNAfold.cgi were consulted during probe design. The study was performed using antisense DNA oligonucleotide probes. The following DNA oligonucleotides were used: *PoptrCAD4* > estExt_Genewise1_v1.C_LG_IX2359, 5′BiotinATTCAACTTTTTCTTTATTTTAAAAGCAAAGAC3′; *PoptrCAD10* (grail3·0004034803) and 5′BiotinTCTATTTATTCATCACAACAACACATGT3′.

Harvested segments of pioneer roots (from the same root fragments as for TUNEL analyses) were fixed immediately in 4 % formaldehyde overnight and then material was rinsed three times with PBS (0·01 m; Sigma), dehydrated in a graded ethanol series (10–100 %) and finally infiltrated and embedded in Paraplast Extra (melting point = 50 °C; Sigma). Sections (12 μm) were prepared with a HM 340E rotary microtome (Microm). The Tyramine Signal Amplification System (TSA; Invitrogen, Carlsbad, CA, USA) was used to enhance the fluorescence *in situ* hybridization (FISH) signal. Probes for FISH were prepared by adding a single biotin residue to the 5′ end of each DNA probe fragment (Genomed, Warsaw, Poland). For hybridization, the probes were resuspended in hybridization buffer (30 % formamide (v/v), 4 × SSC, 5 × Denhardt's buffer, 1 mM EDTA and 50 mM phosphate buffer) to a concentration of 50 pmol. *In situ* hybridization was carried out as described previously (Smoliński *et al*., 2007). Hybridization was performed overnight at 28 °C. All biotin-labelled probes were detected after hybridization using streptavidin–horseradish peroxidase and either Alexa Fluor 488 or Alexa Fluor 546 tyramine (in accordance with the Invitrogen MP 20911 protocol). Finally, the slides were stained using DAPI (4′,6-diamidino-2-phenylindole, 1 μg mL^{-1} for 3 min), washed in double-distilled water and mounted in Citifluor glycerol solution (Agar Scientific, Stansted, UK). For the *in situ* hybridizations, sense-labelled probes and RNase-treated samples were used. For the negative control, we used sense samples because the probes were antisense. In addition, antisense probes were digested with RNase. All control reactions produced negative or negligible results compared with those of standard reactions. Root sections were examined with a Nikon Eclipse 80i fluorescence microscope (Nikon Corporation, Tokyo, Japan). The CPI Plan Fluor × 40 (numerical aperture 1·3) oil immersion lens and narrow excitation band longpass barrier filters (UV-2EC, G-1B and B-1A) were used. The results were recorded using a Nikon DS-5Mc digital camera and LUCIA GENERAL software (Laboratory Imaging, Praha, Czech Republic).

RESULTS

Sequence of events of primary xylem differentiation in P. trichocarpa *roots grown under field condition*

On the first day of pioneer root growth, only the procambial tissue was observed in the meristematic zone, regardless of distance from the root tip; however, at the end of first day of pioneer root growth, a few elongated cells appeared at the site of subsequent xylem. Procambial cells of the outermost xylem initials were then located in a tetrarchic arrangement in places where xylem will be subsequently differentiated (Fig. 2). Primordial TEs were detected later in the same areas, opposite still undifferentiated cells under the pericycle (Fig. 3A). First lignified cell walls of the protoxylem were seen at the end of the second day (Figs 2 and 3B). On the third–fourth day of root development, four xylem poles were formed with at least ten vessels with lignified cell walls (Figs 2 and 3C, D). On the fifth–seventh days, the xylem poles expanded laterally, and the cell walls of the TEs underwent intensive lignification (Fig. 2). At this stage, the first cambial cells (secondary meristem) were seen; thus, the main cellular events were investigated up to the fourth day – to ensure that they are closely connected to primary not secondary xylogenesis.

The same cellular events accompanying TE differentiation can be observed at various ages of root growth as differentiating vessels are present in the primary xylem until the seventh day of root growth (Fig. 2). Serial sections of pioneer roots at different ages revealed that this is the best model for studying primary xylogenesis *in planta* when series of developmental stages can be observed at one point time (Fig. 2). The differentiation of protoxylem starts later but mature vessels are observed earlier than in metaxylem, thus we mainly focused on this xylem region, also having the opportunity to observe most xylogenesis events within the same root segment. In this work, we propose to determine the developmental stages of xylem from meristematic tissue (stage 0) through differentiating TEs (primordial TEs, stage 1; and non-functional TEs, stage 2) to fully functional vessels (stage 3).

Detection of DNA fragmentation by the TUNEL assay and cytological observation of nuclei during tracheary element differentiation

Detection of nuclear DNA fragmentation assessed by the TUNEL assay revealed that changes occurred within the nucleus before synthesis of the secondary cell wall. To analyse properly the developmental stages of cells with TUNEL-positive nuclei in roots of different ages, the same corresponding tissues were stained with Safranin O and Fast Green (Fig. 3A–D). The first TUNEL-positive nuclei which appeared were observed at each xylem pole, facing the endodermis, of the tetrarch root in non-lignified thin-walled elongated cells (stage 1, Fig. 3E), that will undergo differentiation into TEs at the beginning of the second day of root growth. No lignin autofluorescence was observed at these poles at the outer edge of the stele in differentiating xylem cells (Fig. 3E–G). However, in the later stage when strong lignin

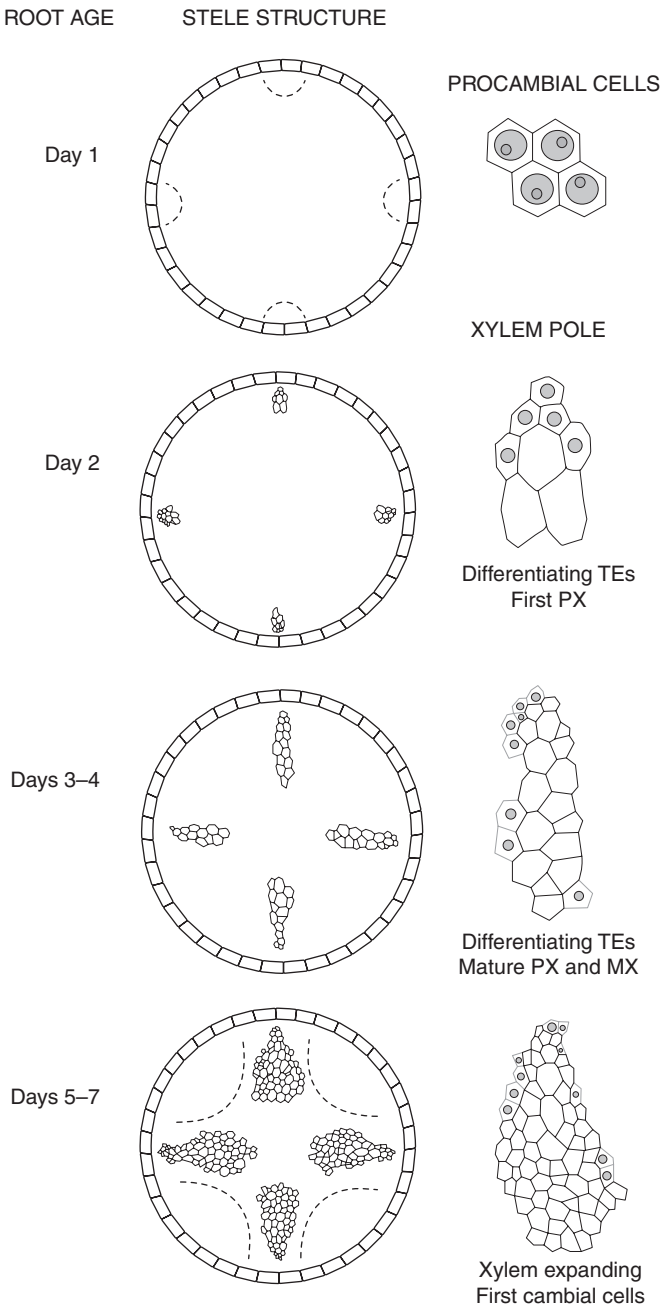

FIG. 2. Stele structure for each day of pioneer root growth (left column) and the area of xylem pole, demonstrating tracheary elements (TEs; empty cells) and primordial differentiating TEs (with nuclei; only those with TUNEL-positive reaction are marked) in root of different ages. Only cells from the meristematic zone are presented at day 1 (in the right column). Both the procambial region of the outermost xylem initials and the first cambial cells are indicated by the dashed line. PX, protoxylem; MX, metaxylem. Note: the figure is not drawn to scale.

autofluorescence as well as a Safranin-positive reaction were noted in the already differentiated TEs, a TUNEL-negative reaction was evident in TEs (Fig. 3B, H). The same pattern was observed both on the second day of root growth (Fig. 3E–H), when xylem formation had been initiated, and on the third–fourth days (Fig. 3I–L), when the first conductive (i.e. fully functional) TEs were observed, as noted in our previous study (Bagniewska-Zadworna *et al.*, 2012). In the older segments of the root, xylem also expands laterally in the stele, and TUNEL-positive nuclei were observed on the sides of the xylem poles in these precursor cells and non-lignified cells (Fig. 3J–L); however, they were not seen in the mature already differentiated TEs with extensively lignified xylem cells (Fig. 3I–K). Safranin staining also revealed relatively large size nuclei at the same sites as where the TUNEL signal was seen (Fig. 3D vs. Fig. 3I–L). With initiation of root secondary growth, when the xylem poles elongated and expanded laterally, the strongly lignified tissue nuclei were TUNEL negative, even if remnants of the protoplasts were present.

Quantitative analyses revealed that on the second day of roots growth, TUNEL-positive nuclei were detected in $2{\cdot}42 \pm 016$ cells (per xylem pole) with thin cell walls without lignin autofluorescence (stage 1) compared with no TUNEL-positive reaction in the already lignified cells (stage 2). On the third–fourth day, TUNEL-positive nuclei were seen in $3{\cdot}71 \pm 0{\cdot}34$ unlignified cells (per xylem pole) and only in $0{\cdot}45 \pm 0{\cdot}15$ already lignified TEs (stages 2–3). These differences were statistically significant ($P < 0{\cdot}001$). At the same time, the number of TEs with lignified cell walls per xylem pole amounted to $4{\cdot}67 \pm 0{\cdot}13$ at the end of the second day and $10{\cdot}58 \pm 0{\cdot}42$ on the third–fourth day of root growth.

Changes in nuclear ultrastructure during xylogenesis were analysed by TEM from the stage of meristematic procambium (stage 0) cells through all stages of non-functional TE formation (stages 1–2; Fig. 4). In the procambium cells of the first day of root growth, the nuclear organization was true to type, with each cell containing one not very compact nucleolus and a small amount of dense, rather scattered chromatin. The nucleus of each meristematic cell was located in the centre of the cell, had a circular outline and was surrounded by a double membrane envelope (Fig. 4A). The differentiating cell gradually became increasingly vacuolated; first small lytic vacuoles accumulated (Fig. 4B), followed by the formation of a large central vacuole (Fig. 4C). In developing TEs (stage 1) a gradual change in the location of the nucleus to a more peripheral position (Fig. 4B, C) and elongation of the nucleus were noted. Nucleoli were more compact than in the procambium, and the nuclear envelope remained intact (Fig. 4B, C). Only in non-functional vessels, in which the secondary cell wall had formed, was the nucleus either undetectable or only partially visible after tonoplast rupture and endonuclease release (stage 2; Fig. 4D).

Histochemical localization of hydrogen peroxide and nitric oxide

The pattern of H_2O_2 localization during vascular differentiation was highly dependent on the cell type and the stage of xylem TE formation; thus, additional staining of the same developmental stages with Safranin O and Fast Green was performed (Fig. 5A–C). H_2O_2 was not detected in the isodiametric and longish procambial cells in either transverse or longitudinal sections during the first day of root growth. A strong colour reaction, which was indicative of a burst of H_2O_2 production, was observed in the differentiating cells and in the first newly established protoxylem TEs (stage 2) with annular or helical cell wall thickenings (Fig. 5D, E). In addition, H_2O_2 was present in the living cells directly adjacent to differentiating or already differentiated vessels (Fig. 5D). Associated with acquisition of the ability to conduct water by TEs and disappearance of their lateral walls, H_2O_2 was detected only in the youngest formed TEs and living

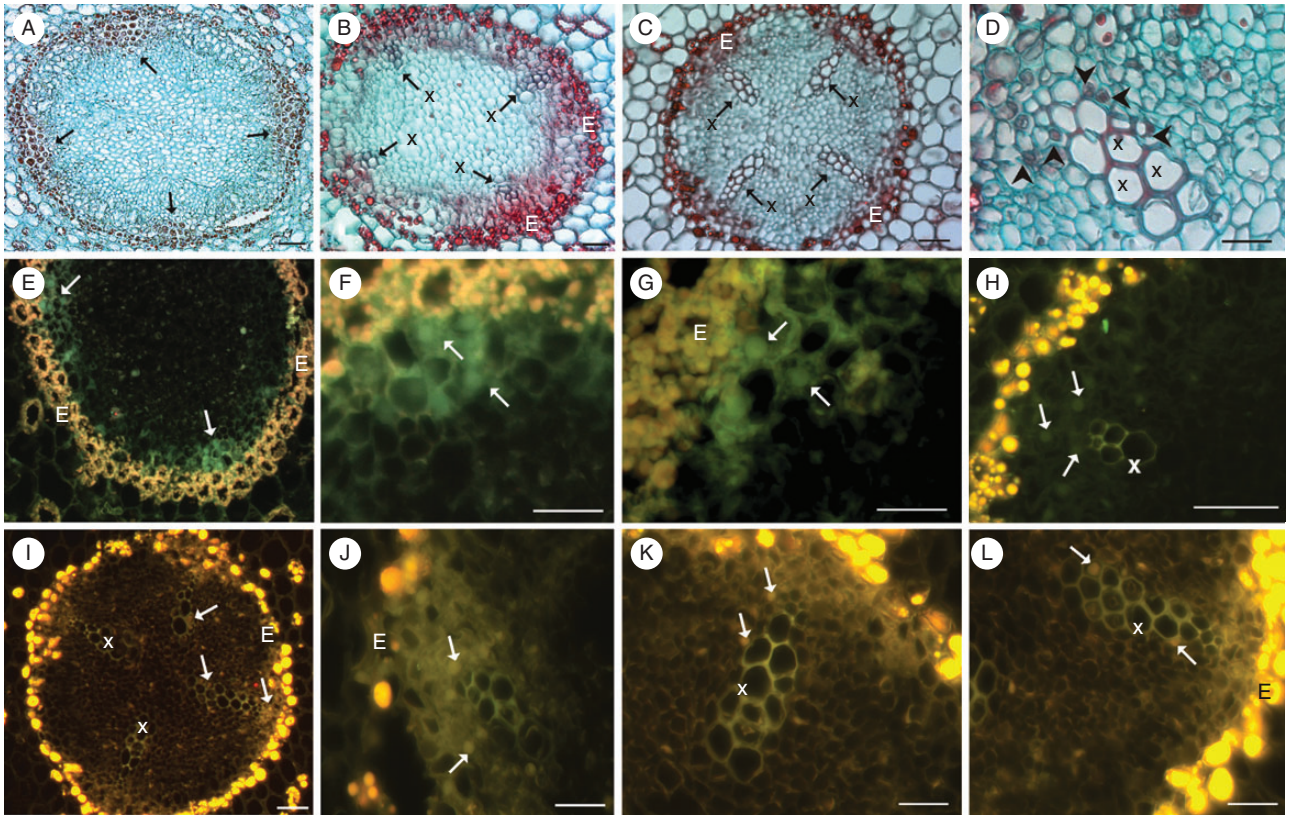

FIG. 3. (A–D) Pioneer root comparative anatomy (transverse sections stained with Safranin and Fast Green). Only undifferentiated cells are located at the sites of subsequent xylem (arrows) and tracheary elements (TEs) are lacking in the stele of 1-day-old roots (A). The first TEs located in four xylem poles of 2-day-old roots (B). Well-developed primary xylem in 3- to 4-day-old roots (C, D). Note the large nuclei in the thin-walled cells, adjacent to mature vessels (D; arrowheads). (E–L) Visualization of nuclear DNA fragmentation through detection of TUNEL-positive nuclei (arrows) during xylogenesis on the second (E–H) and third–fourth days (I–L) of growth of pioneer roots. Note that no TUNEL-positive nuclei were seen in the mature, already differentiated vessels (x). E, endodermis; x, primary xylem. Scale bars = 50 μm.

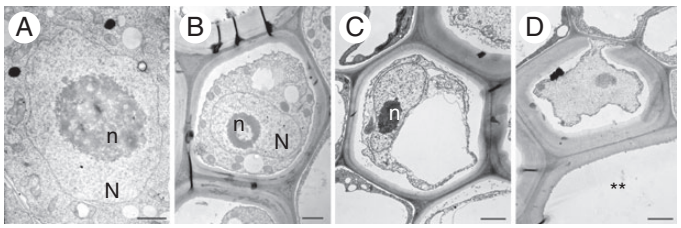

FIG. 4. Nuclear ultrastructure during xylogenesis of *P. trichocarpa* pioneer roots from meristematic cells of the first day of pioneer root growth at stage 0 (A) to initially differentiating primordial tracheary elements (TEs) – stage 1 (B, C), and non-conductive xylem vessels – stage 2 (D), as well as mature TEs – stage 3 (D, asterisks) seen from the second to fifth day of root growth. N, nucleus; n, nucleolus. Scale bars (A, B) = 1 μm; (C, D) = 2 μm.

cells bordering TEs (Fig. 5F, G). H_2O_2 was mostly detected in the small diameter vessels with spiral thickenings; however, it was not seen in mature proto- and metaxylem (stage 3) with pitted thickenings (Fig. 5F, G).

Nitric oxide was detected from the initial stages of xylogenesis to all stages of xylem differentiation (Fig. 5H–Q, stages 1–2). At first, NO was detected in longitudinal sections of only slightly elongated single cells, that ceased dividing on the first day of root growth at the site where the innermost xylem formation will occur (Fig. 5H) and was apparent later in the same site in all elongated cells (Fig. 5I, J). In these elongated cells of stage 1, only thin non-lignified cell walls, with still visible end walls, were observed (Fig. 5I, J). At this stage of xylogenesis (first day of root growth), no other symptoms of xylogenesis, such as H_2O_2 deposition, cell wall lignification or changes in the ultrastructure indicating PCD, were apparent. Later a burst of NO production accurately reflected the location of subsequent xylem or was concentrated in bands at the sites of secondary cell wall thickening (Fig. 5K–M). In transverse section, the NO generation was observed precisely at the four subsequent xylem poles of the tetrarch pioneer root (Fig. 5O, P). Other cells of the vascular cylinder did not show NO generation at the same time (Fig. 5O). Subsequently, NO gradually disappeared once lignin had been deposited in the conductive vessels and cell wall thickenings were observed (Fig. 5N, Q).

Localization of cinnamyl alcohol dehydrogenase gene expression

We used FISH to determine precisely the location of transcripts in pioneer roots that express *CAD* genes at different stages of xylogenesis (Figs 6 and 7). On the first day of root growth, when TEs are absent, the expression of *CAD* genes was not seen in the procambial cells of stage 0. For both *PoptrCAD4* and *PoptrCAD10* genes, the only visible signal was observed in the single cells, highly vacuolated with nuclei

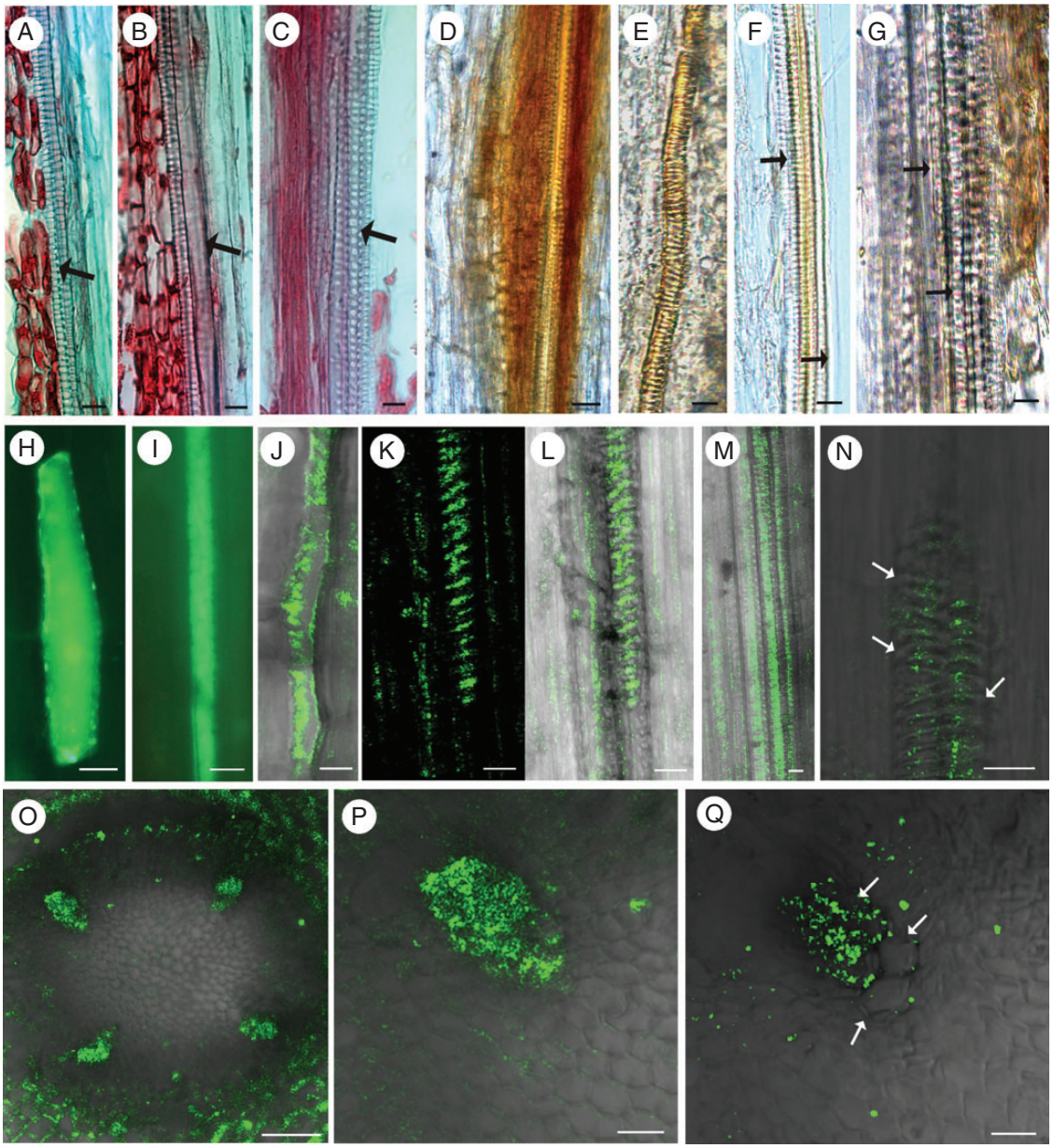

FIG. 5. Pioneer root stele comparative anatomy of consecutive root segments (longitudinal sections stained with Safranin and Fast Green) showing all stages of the first tracheary elements in primary xylem development (A–C, arrows), and stages corresponding to those used for bioimaging of hydrogen peroxide (H_2O_2; D–G) and nitrogen oxide (NO; H–Q) during xylogenesis. Detection of H_2O_2 (DAB positive, represented by red-brown staining) in differentiating tracheary elements on the second day of root growth, in protoxylem vessels with annular or helical cell wall thickening (D, E) and in living cells directly adjacent to differentiating cells on the second day (D) or already differentiated vessels of 3-day-old roots (G). Note that H_2O_2 was not detected in large diameter functional vessels of stage 3 (F, G; arrows). Initial NO accumulation [represented by green fluorescence of the triazole molecule (DAF-2 T) formed from DAF-2DA] in single cells at the site of subsequent xylem formation on the first day of root growth (H–J), and NO appearance in the various stages of differentiating xylem on the second and third day of root growth (K–Q). Note the NO burst in non-lignified thin-walled cells with end walls visible – stage 1 (H–J) and the gradual disappearance of NO in the mature thick-walled xylem vessels – stage 3 (N, Q; arrows). Scale bars (A–N, P, Q) = 10 μm; (O) = 50 μm.

located along the cell walls that are not always expected to be stage 1 of differentiated first protoxylem TEs (Fig. 6C, G). Analysis by FISH using specific probes for *PoptrCAD4* and *PoptrCAD10* (xylem-specific markers selected for *Populus* by Barakat *et al*., 2009) revealed that both of the genes analysed were expressed in the same areas of the root and in the same cell types (Fig. 6). Expression was limited to each xylem pole in sites facing the endodermis (Fig. 6I, K, O). Expression was detected at stage 1 in elongated cells of primordial TEs and in the thin-walled cells directly adjacent to the xylem pole, with the strongest signal coming from nuclei. Also later in development strong signal was observed in the nuclei of differentiating xylem cells (Fig. 7A). A lack of expression was noted in the cells of stages 2 and 3 when lignin deposition occurred (Figs 6K, O and 7A). Expression of the genes analysed was xylem pole specific and was not observed in other cell types

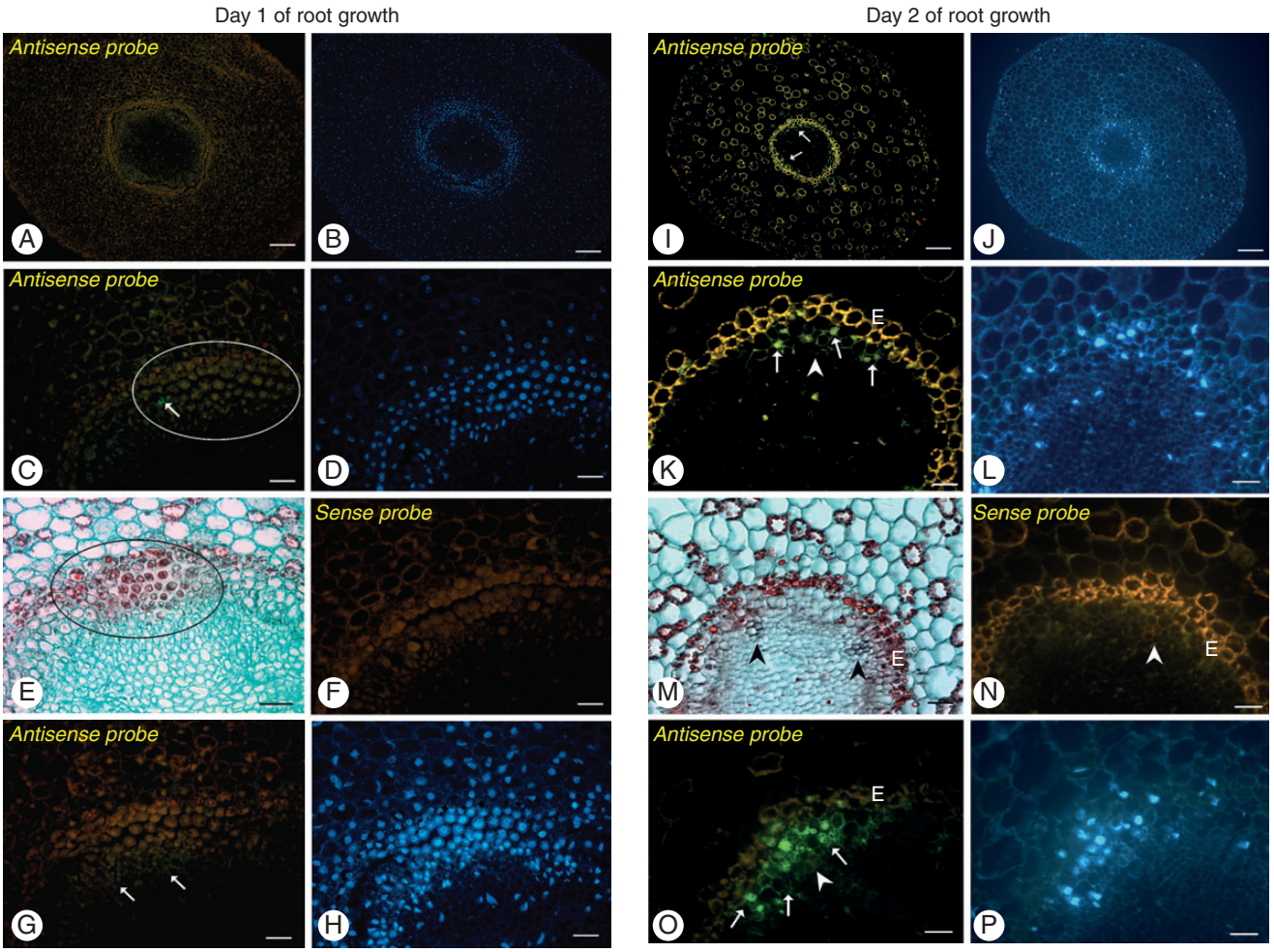

FIG. 6. Fluorescent *in situ* hybridization with *PoptrCAD4* (A–F, I–N) and *PoptrCAD10* (G, H, O, P) probes on the first vs. the second day of root growth. Hybridization signal is visible as green fluorescence (Alexa 488, arrows). To visualize the lack (E) or the degree of xylem differentiation (M), the same root segments as analysed for FISH were observed using light microscopy on sections stained with Safranin and Fast Green. In addition, DAPI staining was used to visualize nuclei (B, D, H, J, L, P). First non-functional xylem vessels are indicated by arrowheads; slight lignin autofluorescence is visible in red. Note the lack of hybridization signal in the undifferentiating cells (encircled) on the first day of root growth and in the protoxylem vessels, and the positive hybridization signal in the first primordial TEs and in the thin-walled cells adjacent to the xylem pole (arrows). Control experiments using sense probes did not result in significant signals in any structure (F, N). E, endodermis. Scale bars (A, B, I, J) = 100 μm; (C–H, K–P) = 50 μm.

within vascular cylinders with the exception of the cells adjacent to the xylem pole at the same time point (Fig. 6I, K, O). Additionally, to check if the expression signal comes from the nuclei, images after DAPI staining were also analysed (Figs 6 and 7), and for each gene analysed and each tissue after sense probe treatment, no expression was detected (Fig. 6). The same pattern of expression was seen independently of the kind of fluorophore used.

A summary of all cellular events leading to the formation of primary xylem tissue, with the TE stage of differentiation indicated, is presented in Fig. 8.

DISCUSSION

In higher plants, a well-organized root system is responsible for water and nutrient uptake from the soil, which is of crucial importance for whole-plant functioning. Woody plants achieve this function by forming pioneer roots, which act as organs to receive water from fibrous roots and facilitate long-distance transport of water to the above-ground tissues (Polverigiani *et al.*, 2011; Zadworny and Eissenstat, 2011; Bagniewska-Zadworna *et al.*, 2012). Knowledge of root structure and function is important because roots influence the course of the transpiration stream and resistance to water movement, and the ability of root systems to expand affects the volume of soil available as a source of water and mineral nutrients. In a previous study, by examining the development of TEs daily in black cottonwood first-order roots, we were able to identify all stages of xylogenesis, which indicated that the rate of xylem vessel differentiation differed between pioneer and fibrous roots (Bagniewska-Zadworna *et al.*, 2012). In *P. trichocarpa*, initial TEs form much closer to the root tip (on the first day of root growth) in fibrous roots than in pioneer roots. Given that TEs of pioneer roots start to mature on the second day of growth and at greater distances from the root tip than in fibrous roots, pioneer roots are perfect research material for analysis of all stages of xylogenesis. In pioneer roots, no visible changes in the structure of meristematic tissue are evident on the first day

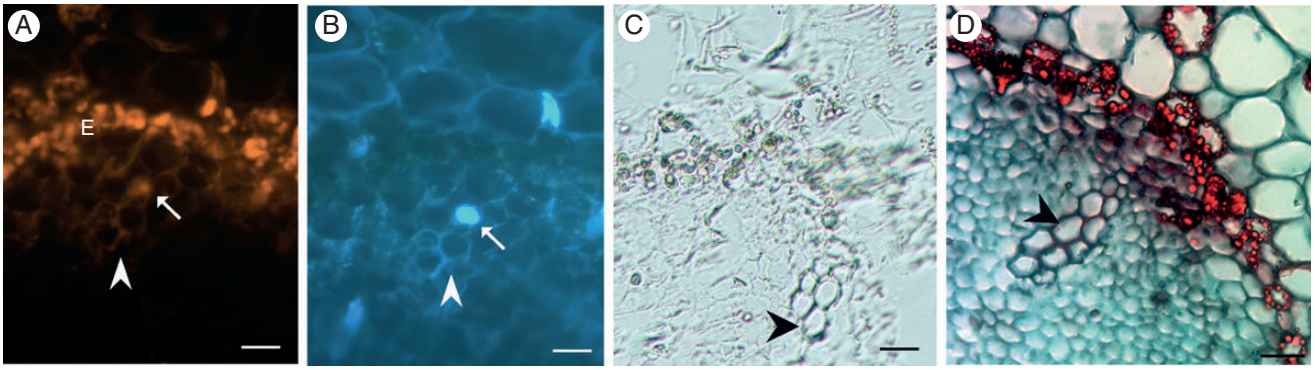

FIG. 7. Fluorescence *in situ* hybridization with *PoptrCAD10* probes on the third day of root growth. Hybridization signal in the cells of stage 1 is visible as yellow fluorescence (A; Alexa 546, arrows). DAPI staining (B) was used to detect nuclei, and bright field imaging (C) as well as Safranin and Fast Green staining (D) were used to visualize mature xylem cells with secondary cell walls (black arrowheads). Note the lack of hybridization signal in the developed tracheary elements – cells of stages 2 and 3 (arrowhead). Scale bars = 50 μm.

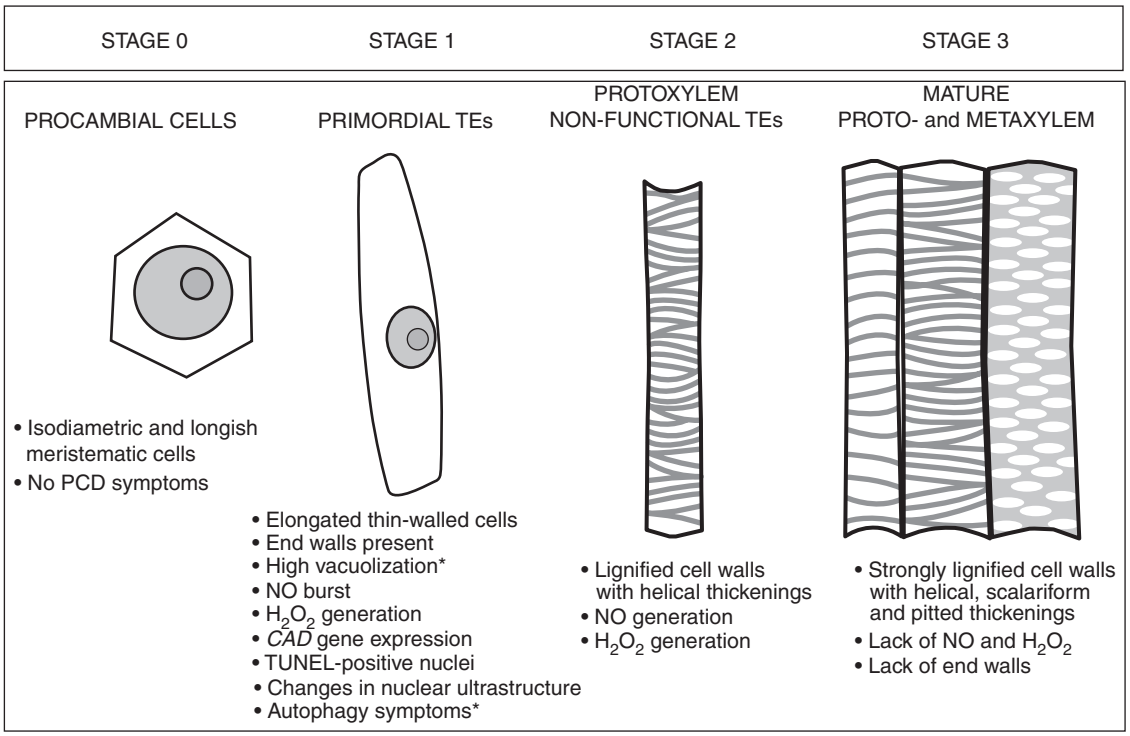

FIG. 8. Sequence of events during primary xylogenesis in pioneer roots of *Populus trichocarpa*. Data originate from this work and a previous study by Bagniewska-Zadworna *et al*. (2012) (marked by asterisks). Note: the figure is not drawn to scale.

of growth. Differentiating TEs are easily recognized on the second day, only primary xylem is observed on the third–fourth days and cambium has been initiated and secondary growth is underway on the sixth–seventh days (Bagniewska-Zadworna *et al*., 2012). In the present study, we used the same well-defined developmental stages to examine whether xylogenesis events under field conditions differ from those described for *Z. elegans in vitro* suspension cultures after the cultures are forced to undergo transdifferentiation (Groover *et al*., 1997; Fukuda, 2000; Kuriyama and Fukuda, 2001; Obara *et al*., 2001; Fukuda, 2004). This approach provides the real possibility to provide the details of the sub-cellular sequence of events during primary xylogenesis in pioneer roots.

As in animals, PCD in plants is frequently characterized by the fragmentation of nuclear DNA. TUNEL-positive cells are observed during PCD in reproductive tissue development, for example during nucellus degeneration (Greenwood *et al*., 2005), plant embryo abortion (Filonova *et al*., 2002), and pollen tube PCD during self-incompatibility (Jordan *et al*., 2000; Thomas and Franklin-Tong, 2004). TUNEL-positive cells are also detected during leaf senescence (Yen and Yang, 1998), the formation of short-lived tracheid rays (Nakaba

et al., 2011), xylogenesis of pea plants (Mittler and Lam, 1995) as well as in plant response to abiotic and biotic stresses, i.e. cadmium-induced PCD in roots (Arasimowicz-Jelonek *et al*., 2012) and the hypersensitive response caused by pathogen infection (Floryszak-Wieczorek *et al*., 2007). Given the prevalence of DNA degradation during PCD, it is astonishing that nuclear fragmentation and/or chromatin condensation were not generally observed during the initial stages of TE formation during transdifferentiation in *Zinnia in vitro* suspension cultures (Groover *et al*., 1997; Obara *et al*., 2001). In contrast, DNA fragmentation was observed at the comparable stage of secondary xylem development (Cao *et al*., 2003; Courtois-Moreau *et al*., 2009). In review papers, Van Doorn (2011) and Van Doorn *et al.* (2011) cite examples where DNA degradation, chromatin aggregation and movement of condensed chromatin to the periphery of the nucleus, nuclear envelope disassembly and finally break up of the nucleus into smaller fragments generally occur before tonoplast rupture during autophagy in plants. It was postulated that in *Zinnia*, commencement of DNA degradation coincides with or immediately follows endonuclease release from the vacuole (Obara *et al*., 2001). However, in the present study, TUNEL-positive nuclei were generally not detected in strongly lignified xylem cells; on the contrary, they were observed at each of the xylem poles, facing the endodermis, during early cell differentiation. The same pattern of DNA degradation was visible in the differentiating TEs on the second day of root growth, when functional xylem had not yet formed, and on the third–fourth days, when the first conductive TEs were observed. Furthermore, xylem in the older segments of the root also expands laterally in the stele, and TUNEL-positive nuclei were observed in these precursor cells. Similarly, during observation of PCD in short-lived pine tracheid rays, TUNEL-positive nuclei were detected first in the ray tracheids located close to those that had already died (Nakaba *et al*., 2011). On the other hand, during secondary xylem development in poplar wood, nuclear DNA fragmentation was observed early during fibre maturation (Courtois-Moreau *et al*., 2009). In the light of a more recent study (Pesquet *et al*., 2013), showing that TUNEL-positive nuclei were observed prior to lignification in *Zinnia in vitro* TEs and then were absent in lignifying TEs, which is consistent with our results, it is clear that xylogenesis *in vitro* might not really differ in this feature from that in natural conditions.

Thus, the sequence of xylogenesis events in both root and shoot development (Courtois-Moreau *et al*., 2009; Bagniewska-Zadworna *et al*., 2012) shows clearly that cell death is gradual and that mega-autophagy with vacuole collapse and cell autolysis is the last, irreversible definitive step toward cell death, which clears the cell of residual components. Such a scenario does not preclude overlap of previous changes in the nucleus, leading to degeneration. This hypothesis is consistent with the findings of Courtois-Moreau *et al.* (2009), which indicated that nuclear degradation could be gradual and/or slow. Progressive chromatin condensation was observed during hybrid embryo PCD in intergeneric *Salix viminalis* × *Populus* crosses (Bagniewska-Zadworna *et al*., 2010) as well as during xylogenesis in this work. In the present study, changes in nuclear structure were seen by TEM long before secondary cell wall formation and cell death. Similar findings were reported during secondary wood formation in poplar, in which nuclei with irregularly formed outlines were observed in highly vacuolated differentiating cells (Arend and Fromm, 2003). The nucleus is the last recognizable organelle in the protoplast of degenerating hybrid embryos (Bagniewska-Zadworna *et al*., 2010). It is possible that the nucleus is maintained as long as vacuole integrity is not destroyed.

To estimate the early events of xylogenesis, we explored the detection and location of molecules that are considered to be involved in signalling during PCD. H_2O_2 and NO function as signalling molecules during cell death in plants (Neill *et al*., 2002) and are produced in response to a variety of stimuli (Arasimowicz-Jelonek *et al*., 2007). The key question is whether both compounds act as signalling molecules and are generated concurrently during xylogenesis in plants. In the present study we detected NO at the onset of cell differentiation, when no other symptoms of autophagy were observed, long before the appearance of secondary cell wall thickening. In addition, NO generation was found at all stages of vessel maturation but not in mature vessels. Similarly, Gabaldon *et al.* (2005), who studied differentiating xylem in the stem of young *Z. elegans* seedlings, observed a burst of NO at the beginning of this process, which was sustained as long as cell wall synthesis and cell autolysis were in progress. Similar results were found in related experiments with suspension cultures, with an NO burst detected in thin-walled transdifferentiating mesophyll cells (Gabaldon *et al*., 2005). Thus, NO production under both *in vivo* and *in vitro* conditions indicates that this reaction is consistent and independent of the type of cell or plant analysed, and is a typical component of PCD induction in plants.

In the current work, we also observed NO accumulation as bands in differentiating vessels at locations very similar to where cell wall thickening is subsequently deposited. This finding is crucial, because there are data indicating that NO might affect lignin biosynthesis through changes in the activity of enzymes involved in this pathway (Polverari *et al*., 2003; Parani *et al*., 2004), including transcriptional regulation of *CAD* genes (Parani *et al*., 2004). Moreover, Arasimowicz *et al.* (2008) clearly proved that NO is engaged in lignin biosynthesis during wounding stress. The elimination of NO, using an NO scavenger (cPTIO), visibly reduced cell wall lignification. However, there is a need for further work to check whether NO is also engaged in other cellular processes during xylogenesis. Both NO and H_2O_2 are produced concurrently during developmental PCD in the nucellus of *Sechium edule* (Lombardi *et al*., 2010) and during *Zinnia* xylem differentiation (Gomez-Ros *et al*., 2012), which is suggestive of their mutual interaction. It has been suggested that the role of both reactive oxygen species (of which the role of H_2O_2 is crucial) as well as signalling molecules, e.g. NO in PCD induction, is complex and time dependent, with both overlapping and different effects noted among cell types (Zhao, 2007; Love *et al*., 2008). Data from the present study suggest that during primary xylogenesis in roots, H_2O_2 was first generated slightly later than NO, and the signal of both molecules disappeared at the same cell stage of differentiated vessels. The pattern of H_2O_2 localization during vascular differentiation was highly dependent on the cell type and the stage of formation of xylem vessels. These results might indicate that H_2O_2 plays twin roles during xylem formation. First, H_2O_2 might be involved in signalling and play an active role in the induction of cell death. This hypothesis is supported by other data for plant PCD (Neill *et al*., 2002; Gechev and Hille,

2005; Lombardi *et al*., 2010). However, the H_2O_2 burst in non-conductive vessels and the strong reaction in the first newly established protoxylem vessels with annular or helical cell wall thickening suggest a different role for H_2O_2 in xylogenesis. Secondly, H_2O_2 could be used by xylem peroxidases for polymerization of *p*-hydroxycinnamyl alcohols into lignins (Higuchi, 1990; Boerjan *et al*., 2003; Takeuchi *et al*., 2005). Of particular importance in this regard is that the presence of H_2O_2 is characteristic of all living cells directly adjacent to differentiating or already differentiated vessels. In the latter case, these observations are consistent with previous reports that only xylem parenchyma cells deliver H_2O_2 necessary for lignification of xylem cell walls (Ros Barceló, 2005). From the site of biosynthesis, H_2O_2 diffuses into the differentiating xylem vessels where it is required for the polymerization of monolignols into lignin. Ros Barceló (2005) has emphasized that H_2O_2 diffusion from the production sites does not influence the rate of secondary cell wall lignification. Recently Pesquet *et al.* (2013) proved that lignification of TEs could take place after vacuolar cell death.

Lignification, which is one of the final stages of xylem differentiation, occurs mainly during expansion in the thickenings of the secondary cell wall (Donaldson *et al*., 2001). Lignin deposition is carried out in several stages, each of which is preceded by the deposition of cellulose (Fukuda, 1996; Turner *et al*., 2007). In the present study, we sought to identify and check if previously selected marker genes for secondary xylogenesis in *P. trichocarpa* (Barakat *et al.*, 2009, 2010) could be associated with TE differentiation during primary xylogenesis and can be used as markers in future studies of other woody plant species.

The *CAD* genes appear to be involved in primary xylem differentiation and the formation of lignified cell walls in TEs before their maturity. The localization of *CAD* gene expression is of considerable interest in this regard. We initially hypothesized that the highest level of *CAD* gene expression is linked to extensively lignified but still living cells. However, signal strength was distributed differently, and *CAD* transcripts were observed in thin cell-walled cells at the beginning of cell differentiation and shortly before DNA degradation as a TUNEL-positive reaction were noted at the same stage of TE differentiation.

Analysis by FISH revealed that expression of all of the genes examined was observed at the same sites in the stele. Deposition was thus limited to the peaks of each xylem pole once TE differentiation had started and to the cells adjacent to these poles. This result is in agreement with our previous results, which indicate that in differentiating cells, and even in thin-walled differentiating TEs, secondary cell wall components were transferred to the walls by vesicles of the Golgi apparatus and/or endoplasmic reticulum (Bagniewska-Zadworna *et al*., 2012). *In situ* hybridization revealed that the accumulation of *Tracheary Element Differentiation* (*TED*) transcripts was restricted to early differentiating cells or to cells that are expected to differentiate (Fukuda, 1996). A similar pattern was noted by Kim *et al.* (2007) in relation to *CAD* gene expression in developing *Arabidopsis thaliana* plants, in which a few genes were expressed in the vascular sites of very young seedlings and again during the development of lateral roots, which is also associated with predictions of xylogenesis of newly initiated root. In roots of woody plants, this specialization is hypothesized to be closely related to the role of xylem at different stages of its development and the different cellular components of the organized, heterogeneous xylem tissue. In addition, TEs that have undergone PCD might be lignified by receiving monolignols from surrounding undifferentiated cells. It was previously emphasized that the enzymes involved in monolignol biosynthesis are separable from the enzymes involved in the polymerization of monolignols (Takabe *et al*., 2001). It should be noted that many biochemical processes in plants are dependent on the close co-operation of neighbouring cells in tissues. Depriving differentiating and neighbouring cells of contact between them by isolation of mesophyll cells before dedifferentiation (as an additional step, not included *in planta*) can interfere with the investigated processes. In this regard, Hosokawa *et al.* (2001) provided extremely valuable data that indicate that intercellular transportation of monolignols through an *in vitro* medium might occur during xylogenesis of isolated *Zinnia* mesophyll cells. Recently, Pesquet *et al.* (2013) also emphasized that the expression of the lignin monomers was not seen only in the lignifying cells but also in the unlignified cells of *Z. elegans* cell cultures and in living, parenchymatic xylem cells that surround TEs in stems, proving that lignification can also occur 'post-mortem'.

In conclusion, although studies of xylogenesis in *Zinnia* cell suspension cultures take place under extremely controlled and artificial circumstances that are unlike natural field conditions, they are of benefit by providing a major contribution to our understanding of TE formation. However, it remains a challenge to determine whether the same processes occur under field conditions during the development of xylem in plant roots and shoots. Our present experiment chronicles the events of xylogenesis during pioneer root development *in situ* under field conditions. As in a previous investigation (Bagniewska-Zadworna *et al*., 2012), we described the timing of xylogenesis from signalling via NO, through secondary cell wall synthesis and autophagy events that are gradual and initiated long before lignification, to completion of the process with tonoplast rupture and lignification, which are necessary for vessels to take on a conductive function. Further stages of lignification depend on transport of monolignols and H_2O_2 for their polymerization in neighbouring cells. The presented study improves our understanding of developmental PCD during primary xylogenesis *in planta*.

ACKNOWLEDGEMENTS

This work was supported by the Polish Ministry of Science and Higher Education (grant no. NN309007437). We thank the Institute of Dendrology, Polish Academy of Sciences, for access to their poplar experimental field site and Leica confocal microscope, and Julia Minicka for her help with sample preparation for TEM.

LITERATURE CITED

Arasimowicz M, Floryszak-Wieczorek J. 2007. Nitric oxide as a bioactive signalling molecule in plant stress responses. *Plant Sciences* **172**: 876–887.

Arasimowicz M, Floryszak-Wieczorek J, Milczarek G, Jelonek T. 2008. Nitric oxide, induced by wounding, mediates redox regulation in pelargonium leaves. *Plant Biology* **11**: 650–663.

Arasimowicz M, Floryszak-Wieczorek J, Deckert J, *et al.* 2012. Nitric oxide implication in cadmium-induced programmed cell death in roots and signaling response of yellow lupin plants. *Plant Physiology and Biochemistry* **58**: 124–134.

Arend M, Fromm J. 2003. Ultrastructural changes in cambial cell derivatives during xylem differentiation in poplar. *Plant Biology* **5**: 255–264.

Bagniewska-Zadworna A, Wojciechowicz MK, Zenkteler M, Jeżowski S, Zenkteler E. 2010. Cytological analysis of hybrid embryos of intergeneric crosses between *Salix viminalis* and *Populus* species. *Australian Journal of Botany* **58**: 42–48.

Bagniewska-Zadworna A, Byczyk J, Eissenstat DM, Oleksyn J, Zadworny M. 2012. Avoiding transport bottlenecks in a developing root system: xylem vessel development in fibrous and pioneer roots under field conditions. *American Journal of Botany* **99**: 1417–1426.

Barakat A, Bagniewska-Zadworna A, Choi A, *et al*. 2009. The cinnamyl alcohol dehydrogenase gene family in *Populus*: phylogeny, organization, and expression. *BMC Plant Biology* **9**: 15.

Barakat A, Bagniewska-Zadworna A, Frost CJ, Carlson JE. 2010. Phylogeny and expression profiling of CAD and CAD-like genes in hybrid *Populus* (*P.* deltoids × P. *nigra*): evidence from herbivore damage for subfunctionalization and functional divergence. *BMC Plant Biology* **10**: 11.

Barlow PW. 1993. The response of roots and root systems to their environment – an interpretation derived from an analysis of the hierarchical organization of plant life. *Environmental and Experimental Botany* **33**: 1–10.

Boerjan W, Ralph J, Baucher M. 2003. Lignin biosynthesis. *Annual Review in Plant Biology* **54**: 519–546.

Bortner CD, Nicklas BE, Oldenburg NBE, Cidlowski JA. 1995. The role of DNA fragmentation in apoptosis. *Trends in Cell Biology* **5**: 21–26.

Boyce CK, Zwieniecki MA, Cody GD, *et al*. 2004. Evolution of xylem lignification and hydrogel transport regulation. *Proceedings of the National Academy of Sciences, USA* **101**: 17555–17558.

Cao J, He XQ, Wang YQ, Sodmergen, Cui KM. 2003. Programmed cell death during secondary xylem differentiation in *Eucommia ulmoides*. *Acta Botanica Sinica* **45**: 1465–1474.

Courtois-Moreau C, Sjödin A, Pesquet E., *et al*.. 2009. A unique programme for cell death in xylem fibers of *Populus* stem. *The Plant Journal* **58**: 260–274.

Donaldson L, Hague J, Snell R. 2001. Lignin distribution in coppice poplar, linseed and wheat straw. *Holzforschung* **55**: 379–385.

Elmore S. 2007. Apoptosis: a review of programmed cell death. *Toxicologic Pathology* **35**: 495–516.

Filonova L, von Arnold S, Daniel G, Bozhov P. 2002. Programmed cell death eliminates all but one embryo in polyembryonic plant seed. *Cell Death and Differentiation* **9**: 6.

Floryszak-Wieczorek J, Arasimowicz M, Milczarek G, Jeleń H, Jackowiak H. 2007. Only an early nitric oxide burst and the following wave of secondary nitric oxide generation enhanced effective defence responses of pelargonium to a necrotrophic pathogen. *New Phytologist* **175**: 718–730.

Fukuda H. 1996. Xylogenesis: initiation, progression and cell death. *Annual Review of Plant Physiology and Plant Molecular Biology* **47**: 299–325.

Fukuda H. 2000. Programmed cell death of tracheary elements as a paradigm in plants. *Plant Molecular Biology* **44**: 245–253.

Fukuda H. 2004. Signals that control plant vascular cell differentiation. *Nature Reviews Molecular Cell Biology* **5**: 379–391.

Gabaldon C, Gomez Ros LV, Pedreno MA, Ros-Barcelo A. 2005. Nitric oxide production by the differentiating xylem of *Zinnia elegans*. *New Phytologist* **165**: 121–130.

Gechev TS, Hille J. 2005. Hydrogen peroxide as a signal controlling plant programmed cell death. *Journal of Cell Biology* **168**: 17–20.

Gómez-Ros LV, Gabaldón C, Núñez-Flores MHL, *et al*. 2012. The promoter region of the *Zinnia elegans* basic peroxidase isoenzyme gene contains *cis*-elements responsive to nitric oxide and hydrogen peroxide. *Planta* **236**: 327–342.

Greenwood JS, Helm M, Gietl C. 2005. Ricinosomes and endosperm transfer cell culture in programmed cell death of the nucellus during Ricinus seed development. *Proceedings of the National Academy of Sciences, USA* 102: 2238–2243

Groover A, Jones AM. 1999. Tracheary element differentiation uses a novel mechanism coordinating programmed cell death and secondary cell wall synthesis. *Plant Physiology* **119**: 375–384.

Groover A, DeWitt N, Heidel A, Jones A. 1997. Programmed cell death of plant tracheary elements differentiating *in vitro*. *Protoplasma* **196**: 197–211.

Higuchi T. 1990. Lignin biochemistry: biosynthesis and biodegradation. *Wood Science and Technology* **24**: 23–63.

Hishi T. 2007. Heterogeneity of individual roots within the fine root architecture: causal links between physiological and ecosystem functions. *Journal of Forest Research* **12**: 126–133.

Hishi T, Takeda H. 2005. Life cycles of individual roots in fine root system of *Chamaecyparis obtuse* Sieb. *et Zucc*. *Journal of Forest Research* **10**: 181–187.

Hodge A. 2009. Root decisions. *Plant, Cell and Environment* **32**: 628–640.

Hosokawa M, Suzuki S, Umezawa T, Sato Y. 2001. Progress of lignifications mediated by intercellular transportation of monolignols during tracheary element differentiation of isolated *Zinnia* mesophyll cells. *Plant and Cell Physiology* **42**: 959–968.

Jordan ND, Franklin FCH, Franklin-Tong VE. 2000. Evidence for DNA fragmentation triggered in the self-incompatibility response in pollen of *Papaver rhoeas*. *The Plant Journal* **23**: 471–479.

Kaliamoorthy S, Krishnamurthy KV. 1998. Secondary wall deposition in tracheary elements of cucumber grown *in vitro*. *Biologia Plantarum* **41**: 515–522.

Kaneda M, Rensing K, Samuels L. 2010. Secondary cell wall deposition in developing secondary xylem of poplar. *Journal of Integrative Plant Biology* **52**: 234–243.

Kim SJ, Kim KW, Cho MH, Franceschi VR, Davin LB, Lewis NG. 2007. Expression of cinnamyl alcohol dehydrogenases and their putative homologues during *Arabidopsis thaliana* growth and development: lessons for database annotations? *Phytochemistry* **68**: 1957–1974.

Kolesnikov VA. 1971. *The root system of fruit plants*. Moscow: MIR Publishers.

Kuriyama H, Fukuda H. 2001. Regulation of tracheary element differentiation. *Journal of Plant Growth Regulation* **20**: 35–51.

Leśniewska J, Simeonova E, Sikora A, Mostowska A, Charzyńska M. 2000. Application of the comet assay in studies of programmed cell death (PCD) in plants. *Acta Societatis Botanicorum Poloniae* **69**: 101–107.

Lombardi L, Ceccarelli N, Picciarelli P, Sorce C, Lorenzi R. 2010. Nitric oxide and hydrogen peroxide involvement during programmed cell death of *Sechium edule* nucellus. *Physiologia Plantarum* **140**: 89–102.

Love AJ, Milner JJ, Sadanandom A. 2008. Timing is everything: regulatory overlap in plant cell death. *Trends in Plant Science* **13**: 589–595.

Lyford WH. 1980. *Development of the root system of northern red oak (Quercus rubra L.)*. Harvard Forest Paper no. 21. Harvard University, Harvard Forest in Petersham, MA.

Mittler R, Lam E. 1995. *In situ* detection of nDNA fragmentation during the differentiation of tracheary elements in higher plants. *Plant Physiology* 108: 489–493.

Moreau C, Aksenov N, Lorenzo MG, *et al*. 2005. A genomic approach to investigate developmental cell death in woody tissues of *Populus* trees. *Genome Biology* **6**: R34.

Nakaba S, Kubo T, Funada R. 2011. Nuclear DNA fragmentation during cell death of short live ray tracheids in the conifer *Pinus densiflora*. *Journal of Plant Research* **124**: 379–384.

Neill SJ, Desikan R, Clarke A, Hurst RD, Hancock JT. 2002. Hydrogen peroxide and nitric oxide as signalling molecules in plants. *Journal of Experimental Botany* **53**: 1237–1247.

Ning S, Song Y, van Damme P. 2002. Characterization of the early stages of programmed cell death in maize root cells by using comet assay and the combination of cell electrophoresis with annexin binding. *Electrophoresis* **23**: 2096–2102.

Noëlle W. 1910. Studien zur vergleichenden anatomie und morphologie der koniferen wurzeln mitrücksicht auf die systematik. *Botanische Zeitung* **68**: 169–266.

Obara K, Kuriyama H, Fukuda H. 2001. Direct evidence of active and rapid nuclear degradation triggered by vacuole rupture during programmed cell death in *Zinnia*. *Plant Physiology* **125**: 615–626.

O'Brien TP, Thimann KV. 1967. Observation on the fine structure of the oat coleoptile III. *Correlated light and electron microscopy of the vascular tissues.* Protoplasma **63**: 443–478.

Parani M, Rudrabhatla S, Myers R, *et al*. 2004. Microarray analysis of nitric oxide responsive transcripts in *Arabidopsis*. *Plant Biotechnology Journal* **2**: 359–366.

Pesquet E, Zhang B, Gorzsás A, *et al*. 2013. Non-cell-autonomous postmortem lignification of tracheary elements in *Zinnia elegans*. *The Plant Cell* **25**: 1314–1328.

Polverari A, Molesini B, Pezzotti M, Buonaurio R, Matre M, Delledone M. 2003. Nitric oxide-mediated transcriptional changes in *Arabidopsis thaliana*. *Molecular Plant-Microbe Interactions* **16**: 1094–1105.

Polverigiani S, McCormack ML, Mueller CW, Eissenstat DM. 2011. Growth and physiology of olive pioneer and fibrous roots exposed to soil moisture deficits. *Tree Physiology* **31**: 1228–1237.

Roberts K, McCann MC. 2000. Xylogenesis: the birth of a corpse. *Current Opinion in Plant Biology* **3**: 517–522.

Ros Barceló A. 2005. Xylem parenchyma cells deliver the H_2O_2 necessary for lignification in differentiating xylem vessels. *Planta* **220**: 747–756.

Smoliński DJ, Niedojadło J, Noble A, Górska-Brylass A. 2007. Additional nucleoli and NOR activity during meiotic prophase I in larch (*Larix decidua* Mill.). *Protoplasma* **232**: 109–120.

Sperry JS, Stiller V, Hacke UG. 2002. Soil water uptake and water transport through root systems. In: Waisel Y, Eshel A, Kafkafi U, eds. Plant roots: the hidden half*, 3rd edn*. New York: Marcel Dekker, 157–174.

Srivastava LM, Singh AP. 1972. Certain aspects of xylem differentiation in corn. *Canadian Journal of Botany* **50**: 1795–1804.

Sutton RF, Tinus RW. 1983. Root and root system terminology. *Forest Science Monograph* **24**: 1–138.

Takabe K, Takeuchi M, Sato T, Ito M, Fujita M. 2001. Immunolocalization of enzymes involved in lignification. *Progress in Biotechnology* **18**: 177–186.

Thomas SG, Franklin-Tong VE. 2004. Self-incompatibility triggers programmed cell death in *Papaver* pollen. *Nature* **429**: 305–309.

Takeuchi M, Takabe K, Fujita M. 2005. Immunolocalization of an anionic peroxidase in differentiating poplar xylem. *Journal of Wood Science* **51**: 317–322.

Thordal-Christensen H, Zhang Z, Wei Y, Collinge DB. 1997. Subcellular localization of H_2O_2 in plants. *H_2O_2 accumulation in papillae and hypersensitive response during the barley–powdery mildew interaction.* The Plant Journal **11**: 1187–1194.

Turner S, Gallois P, Brown D. 2007. Tracheary element differentiation. *Annual Review of Plant Biology* **58**: 407–433.

Van Doorn WG. 2011. Classes of programmed cell death in plants, compared with those in animals. *Journal of Experimental Botany* **62**: 4749–4761.

Van Doorn WG, Woltering EJ. 2005. Many ways to exit? Cell death categories in plants. *Trends in Plant Science* **10**: 117–122.

Van Doorn WG, Woltering EJ. 2010. What about the role of autophagy in PCD? *Trends in Plant Science* **15**: 361–362.

Van Doorn WG, Beers EP, Dangl JL, *et al*. 2011. Morphological classification of plant cell deaths. *Cell Death and Differentiation* **18**: 1241–1246.

Verdaguer D, Molinas M. 1999. Developmental anatomy and apical organization of the primary root of cork oak (*Quercus suber* L.). *International Journal of Plant Sciences* **160**: 471–481.

Yen CH, Yang CH. 1998. Evidence for programmed cell death during leaf senescence in plants. *Plant and Cell Physiology* **39**: 922–927.

Yorimitsu T, Klionsky DJ. 2005. Autophagy: molecular machinery for self-eating. *Cell Death and Differentiation* **12**: 1542–1552.

Zadworny M, Eissenstat DM. 2011. Contrasting the morphology, anatomy and fungal colonization of new pioneer and fibrous roots. *New Phytologist* **190**: 213–221.

Zenkteler E, Bagniewska-Zadworna A. 2005. Ultrastructural changes in rhizome parenchyma of *Polypodium vulgare* during dehydration with or without abscisic acid pretreatment. *Biologia Plantarum* **49**: 209–214.

Zhao J. 2007. Interplay among nitric oxide and reactive oxygen species. *Plant Signaling and Behavior* **2**: 544–547.